IDENTIFICATION AND VALIDATION OF DAMAGE PARAMETERS FOR ELASTO-VISCOPLASTIC CHABOCHE MODEL

A.   A m b r o z i a k

Gdańsk University of Technology
Faculty of Civil and Environmental Engineering
Department of Structural Mechanics and Bridge Structures
Narutowicza 11/12, 80–952 Gdańsk, Poland

The aim of the paper is to propose an improved procedure of damage material parameters identification of the Chaboche model, coupled with the concept of isotropic damage model proposed by AMAR and DUFAILLY [2]. The proposed approach has been implemented into subroutines of the FE MSC.Marc code, as the user's viscoplastic subroutine UVSCPL, and has been used to perform FE static and dynamic computations. The paper gives a brief description of the Chaboche model including damage. The results are also presented of FE dynamic analyses using the respective UVSCPL subroutine. Analyses have been made for the nickel-based superalloy INCO718 and for steel. The numerical examples prove that the proposed identification approach is effective and the numerical implementation is correct.

Key words: damage, elasto-viscoplastic constitutive model, Chaboche, FEM, MSC. Marc.

1. INTRODUCTION

The identification of material parameters and numerical modelling of material damage by means of continuum mechanics is the subject of the present paper. The continuum damage mechanics deals with the microscale-defined damage variables as an effective surface density of cracks or the density of cavity intersections with a plane. For reference, see e.g. KACHANOV [17] or LEMAITRE [24], where the authors focused on the extensive study of continuum damage mechanics.

Since KACHANOV [18] introduced in 1958 the concept of effective stress to describe the rupture process under creep conditions, many theories of the continuous damage mechanics have been developed, regarding the concept of the isotropic damage variable (see e.g. RABOTNOV [31], HAYHURST and LECKIE [16], LEMAITRE and PLUMTREE [25], LECKIE [21], SIMO and JU [32], FOTIU *et al.* [14], SKRZYPEK *et al.* [33]). In the present paper, the isotropic damage concept is used (see LEMAITRE [23] for details), which defines the surface density of microcracs and microcavities. For the sake of this concept the material damage parameters are specified. This approach is introduced into the FE procedure with the Chaboche model employed.

2. Chaboche model equations

In the 1960s Perzyna [29] proposed the elasto-viscoplastic constitutive model, based on the orthogonal condition in the plastic law. The extension of the Perzyna law is the constitutive model proposed by Chaboche [12]. The Chaboche model is based on the assumption of the strain additivity

$$(2.1) \qquad \dot{\boldsymbol{\varepsilon}} = \dot{\boldsymbol{\varepsilon}}^E + \dot{\boldsymbol{\varepsilon}}^I,$$

where $\dot{\boldsymbol{\varepsilon}}$ is the total strain rate, $\dot{\boldsymbol{\varepsilon}}^E$ is the elastic strain rate and $\dot{\boldsymbol{\varepsilon}}^I$ is the inelastic strain rate.

The isotropic damage expressed by the scalar parameter fulfils the condition $D \in (0, 1)$. Based on the damage model proposed by Kachanov [18], the effective tensor of elasticity $\mathbf{B}^*$ for damaged material may be represented by the standard elasticity tensor $\mathbf{B}$ reduced by the damage parameter

$$(2.2) \qquad \mathbf{B}^* = (1 - D) \cdot \mathbf{B}.$$

Therefore, the relation between the stress and strain rate for the assumed isotropic model of material can be expressed as follows:

$$(2.3) \qquad \dot{\boldsymbol{\sigma}} = (1 - D) \cdot \mathbf{B} : \dot{\boldsymbol{\varepsilon}}^E = \mathbf{B}^* : \left(\dot{\boldsymbol{\varepsilon}} - \dot{\boldsymbol{\varepsilon}}^I \right).$$

Consequently, the nominal stress rate $\dot{\boldsymbol{\sigma}}$ is replaced by the effective stress rate $\dot{\sigma}^*$ in the damaged material, according to the formula

$$(2.4) \qquad \dot{\boldsymbol{\sigma}}^* = \frac{\dot{\boldsymbol{\sigma}}}{1 - D}.$$

Replacing the initial stress by the effective stress in the constitutive equations of the undamaged material makes it possible to consider the case of damage. Therefore the damage evolution D, proposed by Lemaitre [23], is expressed by the equation

$$(2.5) \qquad \dot{D} = \left(\frac{Y}{S} \right)^s \cdot \dot{p}.$$

The variables s and S are the damage material parameters, which are specified on the basis of experimental tests. The rate of the equivalent plastic strain $\dot{p}$ will be specified in the next part of the paper. The function Y is determined by the Young's modulus E, the Poisson's ratio ν and the current values of damage D, the Huber–Mises equivalent stress σ_{eq} and the hydrostatic stress σ_H. This function is called the damage strain energy release rate. It is expressed by the equation

$$(2.6) \qquad Y = \frac{\sigma_{eq}^2}{2 \cdot (1 - D)^2 \cdot E} \cdot \left(\frac{2}{3} \cdot (1 + \nu) + 3 \cdot (1 - 2 \cdot \nu) \cdot \left(\frac{\sigma_H}{\sigma_{eq}} \right)^2 \right).$$

In isothermal conditions, the inelastic strain rate $\dot{\boldsymbol{\varepsilon}}^I$ in the basic variant of the Chaboche model can be expressed by the following formula

$$(2.7) \qquad \dot{\boldsymbol{\varepsilon}}^I = \frac{3}{2} \cdot \dot{p} \cdot \frac{\boldsymbol{\sigma}' - \mathbf{X}'}{J\left(\boldsymbol{\sigma}' - \mathbf{X}'\right)}.$$

The rate $\dot{p}$ is defined by the equation (see e.g. AMAR and DUFAILLY [2])

$$(2.8) \qquad \dot{p} = \left\langle \frac{\dfrac{J\left(\boldsymbol{\sigma}' - \mathbf{X}'\right)}{1 - D} - R - k}{K} \right\rangle^n$$

where k, K and n are material parameters. The material constant k corresponds to the initial yield stress, while the factor R describes the isotropic hardening. Following $\boldsymbol{\sigma}'$ and $\mathbf{X}'$ are the deviatoric parts of stress tensor and back-stress tensor. Additionally, the invariant $J\left(\boldsymbol{\sigma}' - \mathbf{X}'\right)$ is specified as

$$(2.9) \qquad J\left(\boldsymbol{\sigma}' - \mathbf{X}'\right) = \sqrt{\frac{3}{2}\left(\boldsymbol{\sigma}' - \mathbf{X}'\right) : \left(\boldsymbol{\sigma}' - \mathbf{X}'\right)}.$$

The evolution of the isotropic hardening R is defined by

$$(2.10) \qquad \dot{R} = b \cdot (R_1 - R) \cdot \dot{p},$$

while the kinematic $\mathbf{X}$ hardening is described as

$$(2.11) \qquad \dot{\mathbf{X}} = \frac{2}{3} \cdot a \cdot \dot{\boldsymbol{\varepsilon}}^I - c \cdot \mathbf{X} \cdot \dot{p}.$$

The variables b, R_1 and a, c are the material parameters, which have to be specified on the basis of laboratory tests. It should be noted that it is necessary to establish eleven material parameters in the presented model: two elastic parameters E and ν, seven inelastic parameters k, n, K, c, a, b, R_1, and two additional damage parameters S, s.

The detailed description of several variants of the Chaboche model, with the material parameters specified, was given by the present author in [4] and [37]. The constitutive equations of the Chaboche model, with respect to a hierarchy of various models, were presented by CHABOCHE in [12] and WOZNICA in [36]. AKTAA and SCHINKE [1] applied the damage model proposed by HAYHURST [16] to the Chaboche model. In the paper [11] BROCKS and LIN extended the Chaboche viscoplastic law to a finite strain form based on an internal dissipation inequality. The authors assumed a multiplicative decomposition of the deformation gradient into elastic and inelastic parts. In order to numerically investigate the extended viscoplastic law, finite element algorithm and several examples were presented.

3. Application of the Chaboche model to FE open code

In the numerical analysis the MSC.Marc system has been used. It is a multi-purpose, FEA program for advanced engineering simulations, ready to be extended by user's subroutines. In order to apply the Chaboche model to the MSC. Marc system, the user-defined subroutines UVSCPL [34] were applied, with the inelastic strain rate and the stress increments specified. The main part of the algorithm used in the UVSCPL subroutine is presented in the form of a flow chart, in two variants. In Fig. 1 the undamaged Chaboche model is shown and in Fig. 2 the damage is considered. The present author used this UVSCPL procedure for static and dynamic analysis with the Chaboche model (see e.g. [6] and [38]). It should be noted that the values of time functions should be calculated in each step of iteration.
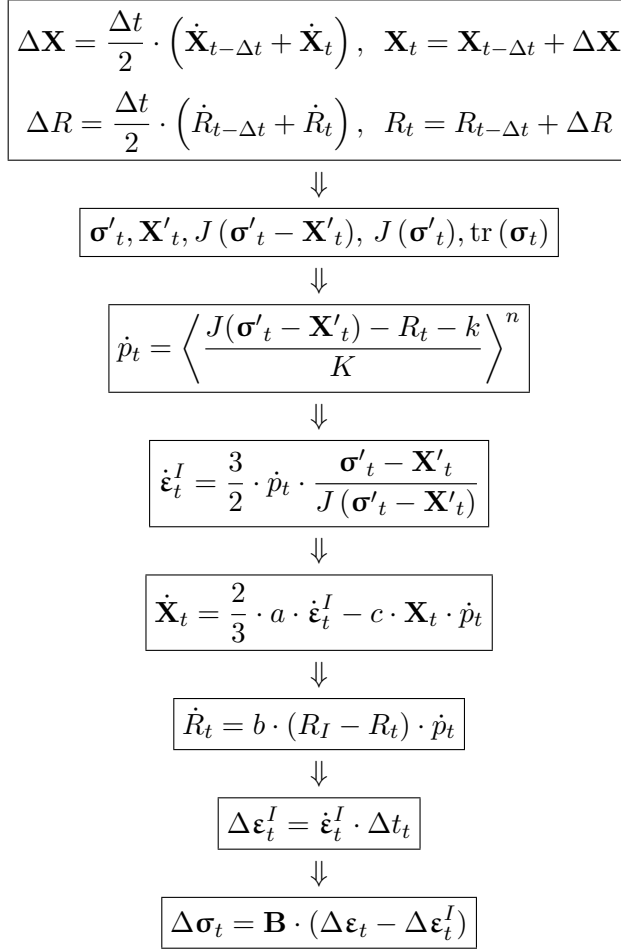
$$\Delta\mathbf{X} = \frac{\Delta t}{2} \cdot \left(\dot{\mathbf{X}}_{t-\Delta t} + \dot{\mathbf{X}}_t \right), \quad \mathbf{X}_t = \mathbf{X}_{t-\Delta t} + \Delta\mathbf{X}$$

$$\Delta R = \frac{\Delta t}{2} \cdot \left(\dot{R}_{t-\Delta t} + \dot{R}_t \right), \quad R_t = R_{t-\Delta t} + \Delta R$$

$$\Downarrow$$

$$\boldsymbol{\sigma'}_t, \mathbf{X'}_t, J\left(\boldsymbol{\sigma'}_t - \mathbf{X'}_t\right), J\left(\boldsymbol{\sigma'}_t\right), \mathrm{tr}\left(\boldsymbol{\sigma}_t\right)$$

$$\Downarrow$$

$$\dot{p}_t = \left\langle \frac{J(\boldsymbol{\sigma'}_t - \mathbf{X'}_t) - R_t - k}{K} \right\rangle^n$$

$$\Downarrow$$

$$\dot{\boldsymbol{\varepsilon}}_t^I = \frac{3}{2} \cdot \dot{p}_t \cdot \frac{\boldsymbol{\sigma'}_t - \mathbf{X'}_t}{J\left(\boldsymbol{\sigma'}_t - \mathbf{X'}_t\right)}$$

$$\Downarrow$$

$$\dot{\mathbf{X}}_t = \frac{2}{3} \cdot a \cdot \dot{\boldsymbol{\varepsilon}}_t^I - c \cdot \mathbf{X}_t \cdot \dot{p}_t$$

$$\Downarrow$$

$$\dot{R}_t = b \cdot (R_I - R_t) \cdot \dot{p}_t$$

$$\Downarrow$$

$$\Delta\boldsymbol{\varepsilon}_t^I = \dot{\boldsymbol{\varepsilon}}_t^I \cdot \Delta t_t$$

$$\Downarrow$$

$$\Delta\boldsymbol{\sigma}_t = \mathbf{B} \cdot \left(\Delta\boldsymbol{\varepsilon}_t - \Delta\boldsymbol{\varepsilon}_t^I\right)$$

Fig. 1. Flow chart of the UVSCPL subroutine – Chaboche model.

$$\Delta \mathbf{X} = \frac{\Delta t}{2} \cdot \left(\dot{\mathbf{X}}_{t-\Delta t} + \dot{\mathbf{X}}_t \right), \quad \mathbf{X}_t = \mathbf{X}_{t-\Delta t} + \Delta \mathbf{X}$$

$$\Delta R = \frac{\Delta t}{2} \cdot \left(\dot{R}_{t-\Delta t} + \dot{R}_t \right), \quad R_t = R_{t-\Delta t} + \Delta R$$

$$\Delta D = \frac{\Delta t}{2} \cdot \left(\dot{D}_{t-\Delta t} + \dot{D}_t \right), \quad D_t = D_{t-\Delta t} + \Delta D$$

$$\Downarrow$$

$$\boldsymbol{\sigma}'_t, \mathbf{X}'_t, J\left(\boldsymbol{\sigma}'_t - \mathbf{X}'_t\right), J\left(\boldsymbol{\sigma}'_t\right), \operatorname{tr}\left(\boldsymbol{\sigma}_t\right), \boldsymbol{\sigma}_{eq}, \sigma_H$$

$$\Downarrow$$

$$\dot{p}_t = \left\langle \frac{\left(J(\boldsymbol{\sigma}'_t - \mathbf{X}'_t)/1 - D_t\right) - R_t - k}{K} \right\rangle^n$$

$$\Downarrow$$

$$\dot{\boldsymbol{\varepsilon}}^I_t = \frac{3}{2} \cdot \dot{p}_t \cdot \frac{\boldsymbol{\sigma}'_t - \mathbf{X}'_t}{J\left(\boldsymbol{\sigma}'_t - \mathbf{X}'_t\right)}$$

$$\Downarrow$$

$$\dot{\mathbf{X}}_t = \frac{2}{3} \cdot a \cdot \dot{\boldsymbol{\varepsilon}}^I_t - c \cdot \mathbf{X}_t \cdot \dot{p}_t$$

$$\Downarrow$$

$$\dot{R}_t = b \cdot (R_I - R_t) \cdot \dot{p}_t$$

$$\Downarrow$$

$$Y_t = \frac{\sigma^2_{eq}}{2 \cdot (1 - D_t)^2 \cdot E} \cdot \left(\frac{2}{3} \cdot (1 + \nu) \cdot + 3 \cdot (1 - 2 \cdot \nu) \cdot \left(\frac{\sigma_H}{\sigma_{eq}} \right)^2 \right)$$

$$\Downarrow$$

$$\dot{D}_t = \left(\frac{Y_t}{S} \right)^s \cdot \dot{p}_t$$

$$\Downarrow$$

$$\mathbf{B}^*_t = (1 - D_t) \cdot \mathbf{B}$$

$$\Downarrow$$

$$\Delta \boldsymbol{\varepsilon}^I_t = \dot{\boldsymbol{\varepsilon}}^I_t \cdot \Delta t_t$$

$$\Downarrow$$

$$\Delta \boldsymbol{\sigma}_t = \mathbf{B} \cdot \left(\Delta \boldsymbol{\varepsilon}_t - \Delta \boldsymbol{\varepsilon}^I_t \right)$$
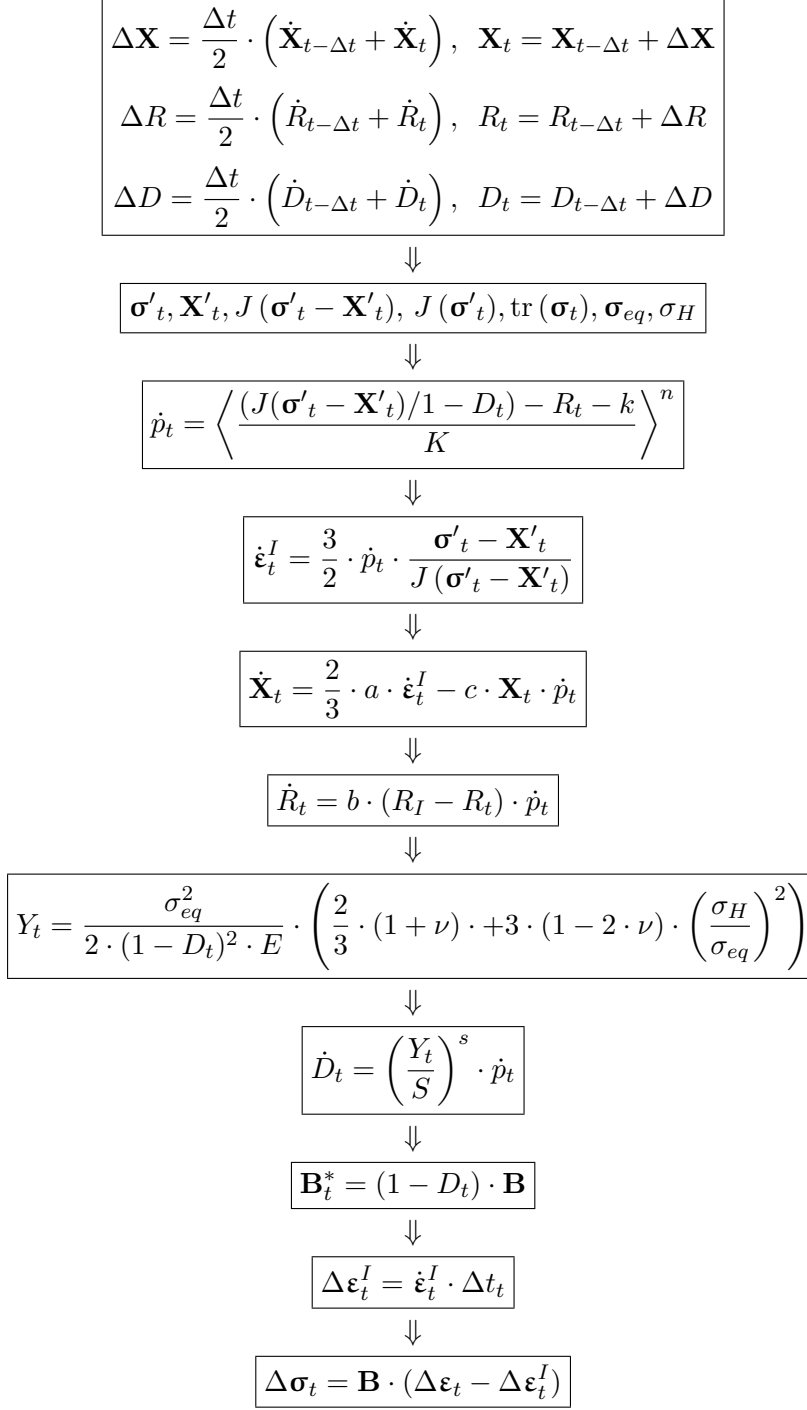
FIG. 2. Flow chart of the UVSCPL subroutine – Chaboche model with damage.

Additionally, at the beginning of a given time step t_i, in the first iteration all values with index t are taken as the final values from the previous step $t_i - \Delta t$.

It should be noted that other commercial FE codes exist; they enable us to introduce the constitutive models defined by the user. For example, some results can be specified of FE analyses. They are the user-defined material models UMAT, in the form of a subroutine introduced to the FE ABAQUS code with the unified viscoplastic model proposed by BODNER and PARTOM [10] and by CHABOCHE [13] for polycrystal alloys, and the creep model suggested by BERTRAM and OLSCHEWSKI [9] for single crystal alloys, coupled with the anisotropic damage model. All these models are presented by QI and BROCK [30].

4. IDENTIFICATION OF DAMAGE PARAMETERS

4.1. Concept of identification

The present author used the concept proposed by AMAR and DUFAILLY [2] in the process of identification of material parameters dealing with damage. In this concept it is assumed that at the beginning of the identification process of damage material parameters the basics constants for the Chaboche model are specified. If the parameters: E, ν and k, n, K, c, a, b, R_1 are known, the damage material parameters can be specified. The detailed description of identification of the material parameters for the Chaboche model is described e.g. by KŁOSOWSKI [19] or AMAR and DUFAILLY [2]. The design of experiments suitable for the parameter identification of the Chaboche material model under the uniaxial loading and stationary temperature conditions has been proposed also by FURAKAWA and YAGAWA [15]. For the detailed studies of experimental methods in material dynamics and impact, the author refers to the work [28].

The material parameters are usually identified on the basis of the uniaxial tension tests. In the case of uniaxial tension tests, the stress tensor $\boldsymbol{\sigma}$ has one non-vanishing component σ

$$(4.1) \qquad \boldsymbol{\sigma} = \begin{bmatrix} \sigma & 0 & 0 \\ 0 & 0 & 0 \\ 0 & 0 & 0 \end{bmatrix},$$

while the Huber–Mises equivalent stress $\sigma_{eq} = \sigma$ and the hydrostatic stress $\sigma_H = \sigma/3$. Then the function of the energy density (Eq. (2.6)) can be rewritten as

$$(4.2) \qquad Y = \frac{\sigma^2}{2 \cdot (1 - D)^2 \cdot E}.$$

For simplicity it has been assumed that rupture of the specimen is specified by the rupture time t_r, while $D = 1.0$. Additionally, in practical applications it is necessary to specify the value of the critical damage D_c, which indicates the limit of the theory. It should be noted that this factor must be lower than 1.0. It usually lies between 0.2 and 0.8, depending on the type of material; see e.g. LEMAITRE [22]. Substituting Eq. (4.2) into Eq. (2.5) we obtain

$$\dot{D} = \left(\frac{\sigma^2}{2 \cdot (1 - D)^2 \cdot E \cdot S} \right)^s \cdot \dot{p},$$

(4.3)

$$\dot{D} \cdot (1 - D)^{2 \cdot s} = \left(\frac{\sigma^2}{2 \cdot E \cdot S} \right)^s \cdot \dot{p}.$$

The author has assumed, as AMAR and DUFAILLY in [2], that the value of the parameter s is chosen arbitrarily; only the factor S has to be determined. Then the interchange of variation is used; the Eq. (4.3) can be transformed to the expressions

$$\int\limits_0^1 (1 - D)^{2 \cdot s} \, dD = \frac{1}{2 \cdot s + 1} = \int\limits_0^{t_r} \left(\frac{\sigma^2}{2 \cdot E \cdot S} \right)^s \cdot \dot{p} \, dt,$$

(4.4)

$$\frac{1}{2 \cdot s + 1} = \left(\frac{1}{2 \cdot E \cdot S} \right)^s \cdot \int\limits_0^{t_r} \sigma^{2 \cdot s} \cdot \dot{p} \, dt \, ;$$

$$(2 \cdot s + 1)^{1/s} = 2 \cdot E \cdot S \cdot \frac{1}{\left(\int\limits_0^{t_r} \sigma^{2 \cdot s} \cdot \dot{p} \, dt \right)^{1/s}}.$$

Finally, we obtain the equation of the damage material parameter S

(4.5)

$$S = \frac{(2 \cdot s + 1)^{1/s}}{2 \cdot E} \cdot \left(\int\limits_0^{t_r} \left(\sigma^{2 \cdot s} \cdot \dot{p} \right) \, dt \right)^{1/s}.$$

We can notice that the parameter S depends on the parameter s and the history of loading (directly on σ and $\dot{p}$). It is necessary to establish the rupture time of the specimen t_r form the uniaxial tensile tests. Additionally it is necessary to obtain the value of the σ_j and $\dot{p}_j$ at each time step. Calculations to the first approximation of the value of the damage parameters have to be performed without damage. To calculate the integral from Eq. (4.5), the present author

used simple method of numerical integration, according to the formula

$$(4.6) \qquad \int\limits_0^{t_r} \left(\sigma^{2\cdot s} \cdot \dot{p} \right) dt = \sum_{j=1}^{n} \left[(\sigma_j)^{2\cdot s} \cdot \dot{p}_j \cdot \Delta t_j \right].$$

Therefore, in the next calculation step, knowing the value of the rupture strain ε_r established in the laboratory test, the parameter S is calculated. The first approximation of the parameter S is made on the basis of the Chaboche model analysis without damage. According to Eq. (4.5), considering the evolution of the stress and $\dot{p}$, the first approximation of the damage parameter S_i is determined. The parameter S is evaluated from the following equation:

$$(4.7) \qquad S_{i+1} = S_i \cdot \frac{\varepsilon_r^{\exp}}{(\varepsilon_r)_i},$$

where $\varepsilon_r^{\exp}$ is the rupture strain, which has been established on the basis of the experimental test; $(\varepsilon_r)_i$ and S_i are the rupture strain and the value of damage parameter S obtained in the i-th iteration of the numerical simulation (index i specifies the number of approximation of the parameter S). In the above concept of identification it is necessary to know the load history and the rupture time t_r, which corresponds to the rupture strain ε_r (leading to the rupture of specimen of the investigated material).

4.2. Identification example – experiment simulation

In this section the present author is basing on the known material parameters for Chaboche model with damage. For these known parameters the author performed simulation of experiments of the uniaxial tensile tests, which are used in the identification process of the damage parameters, according to the concept of identification presented in the preceding section. At the beginning of the identification process of the damage parameters, the author assumed that the basic parameters for Chaboche model are known (E, ν, k, n, K, c, a, b and R_1).

AMAR and DUFAILLY [2] presented the material parameters for nickel-based superalloy INCO718 (at 650° C [2]): $E = 162000.0$ [MPa], $\nu = 0.3$ [$-$], $k = 501$ [MPa], $b = 15.0$ [$-$], $R_1 = -165.4$ [MPa], $a = 80000.0$ [MPa], $c = 200.0$ [$-$], $n = 2.4$ [$-$], $K = 12790$ $\left[(\text{MPa} \cdot \text{s})^{1/n} \right]$, $S = 4.48$ [MPa], $s = 3.0$ [$-$]. On the basis of these material parameters, the authors performed the simulation of the constant strain rate test for $\dot{\varepsilon} = 0.01$ $\left[\text{s}^{-1} \right]$ (see Fig. 3, "Experiment simulation"). The numerical calculation was performed for the truss structure, subjected to the uniaxial tension test. The following geometrical parameters were assumed: length $l = 1.0$ [m] and cross-sectional area $A = 0.001$ [m^2]. It should be noted that failure of the specimen happened suddenly, see Fig. 3.
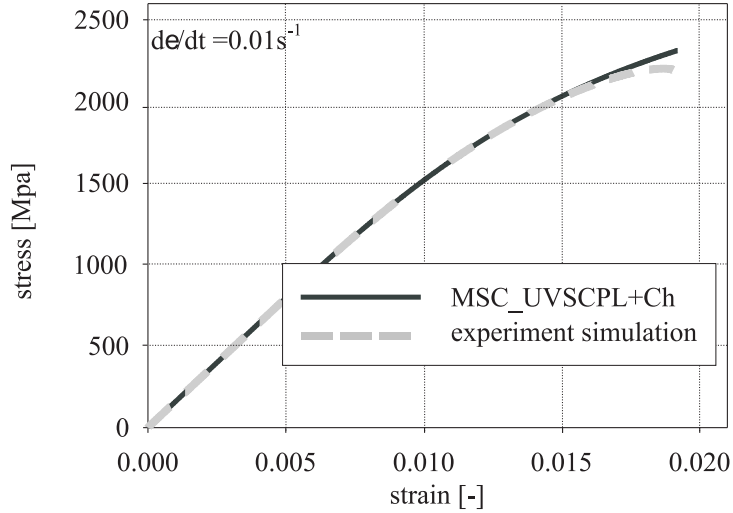
FIG. 3. Constant strain rate test for $\dot{\varepsilon} = 0.01$ s^{-1}.

On the basis of the simulation of experiments performed for the constant strain rate test $\dot{\varepsilon} = 0.01$ $\left[\text{s}^{-1}\right]$, the following rupture time $t_r^{\text{exp}} = 1.92$ [s] (which corresponds to $\varepsilon_r^{\text{exp}} = 0.0192$ [–]) is established. For the purpose of the first approximation of the damage parameters, the author carried out the numerical calculations for the Chaboche model without damage to the limit of the strain $\varepsilon_r^{\text{exp}}$ (see Fig. 3). On the basis of these calculations the evolution of the stress and the rate $\dot{p}$ was specified, see Fig. 4.
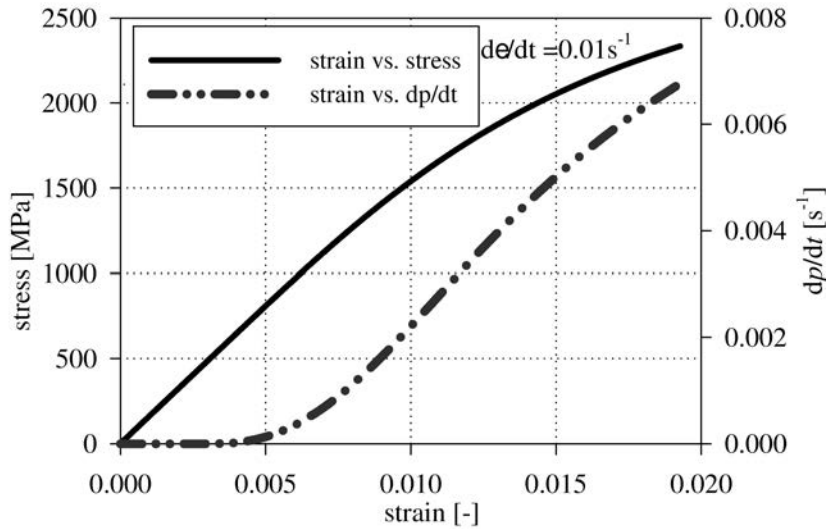
FIG. 4. Stress and $\dot{p}$ in the strain domain for $\dot{\varepsilon} = 0.01$ s^{-1}.

Additionally, at the beginning of the identification process, it was necessary to assume the value of s. In the present investigation the author performed the identification process for five assumed values of parameter s: 1.0; 2.0; 3.0; 4.0; 5.0. In these cases it is possible to observe evolution of the damage material parameters. The values of parameters s may be specified optionally, but the author assumed them to be an integer S (the parameter s is the exponent in the Eq. (2.5)). The first approximation of the parameter S (named S_1 see Table 1), is calculated on the basis of the Chaboche analysis without damage. The following approximation S_i, according to Eq. (4.7), is performed for the Chaboche model coupled with damage. In each step of numerical calculations, strain $(\varepsilon_r)_i$ is specified and compared with the rupture strain obtained from laboratory tests. The results of identification of the damage material parameters are given in Table 1. It is possible to observe that the convergence of the parameter S is better for higher values of the parameter s.

Table 1. Identification of damage parameters.

$s = 1.0$ [–]						
i	1	2	3	4	5	6	7
S_i [MPa]	0.179	0.200	0.219	0.232	0.250	0.260	0.265
$(\varepsilon_r)_i$	0.0170	0.0175	0.0180	0.0183	0.0187	0.0190	0.0191
$s = 2.0$ [–]						
i	1	2	3	4			
S_i [MPa]	1.99	2.10	2.15	2.20			
$(\varepsilon_r)_i$	0.0182	0.0187	0.0189	0.0191			
$s = 3.0$ [–]						
i	1	2	3	5			
S_i [MPa]	4.26	4.33	4.40	4.45			
$(\varepsilon_r)_i$	0.0189	0.0189	0.0190	0.0191			
$s = 4.0$ [–]						
i	1	2					
S_i [MPa]	6.15	6.25					
$(\varepsilon_r)_i$	0.0189	0.0191					
$s = 5.0$ [–]						
i	1	2					
S_i [MPa]	7.62	7.70					
$(\varepsilon_r)_i$	0.0190	0.0192					

For each of the assumed values of the parameter s, parameters S are estimated, see Table 1. For these pairs of damage material parameters, numerical simulation of the uniaxial tension tests for $\dot{\varepsilon} = 0.01\,\mathrm{s}^{-1}$ is performed, see Figs. 5 and 6. In spite of the same rupture strain ε_r specified for each pair of parameters s and S, it is possible to observe small differences between strain vs. stress curves, given in Figs. 5 and 6. These differences can be seen better on the background of the strain vs. damage D curves.
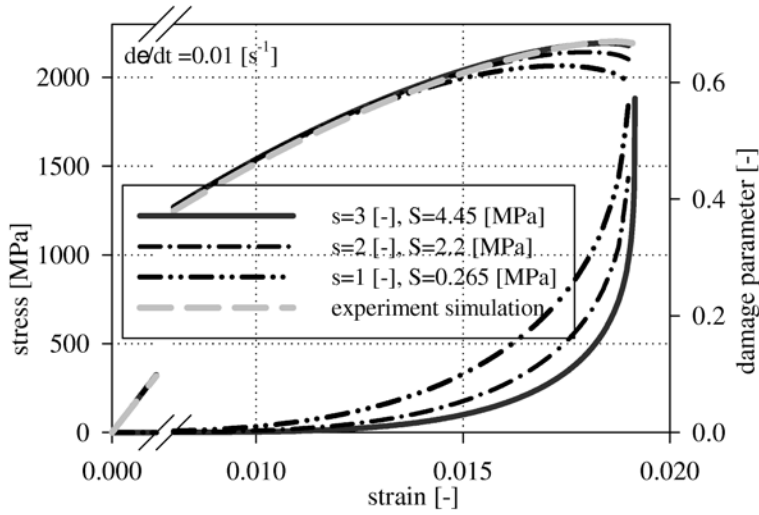
FIG. 5. Simulation of constant strain rate for different values of damage parameters.
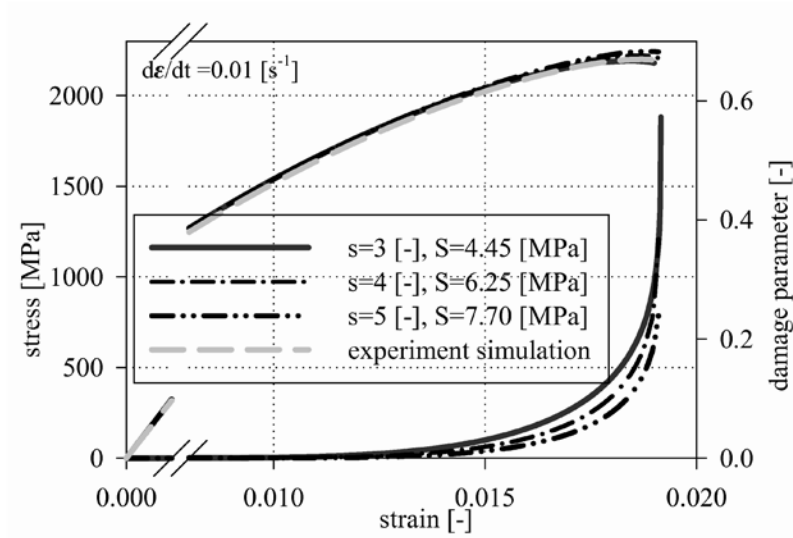
FIG. 6. Simulation of constant strain rate for different values of damage parameters.

For the purpose of final acceptance of pair of damage parameters, simulation of the creep tests (constant stress tests) for $\sigma = 2000$ [MPa] for each pair of the parameters s and S are performed. The obtained results are given in Figs. 7 and 8, where only the numerical calculations with the damage parameters $s = 3.0$ [–] and $S = 4.45$ [MPa] give a good approximation of the simulation of the experiment, see Fig. 9.
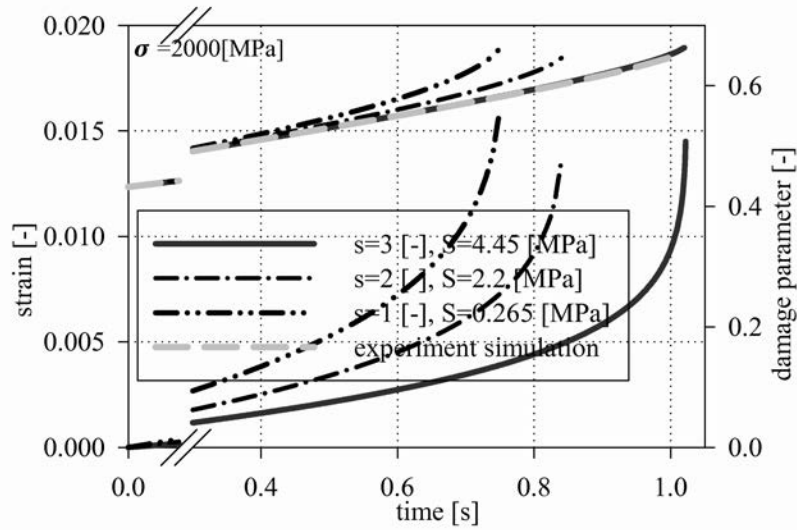
FIG. 7. Creep test for $\sigma = 2000$ [MPa] for different values of damage parameters.
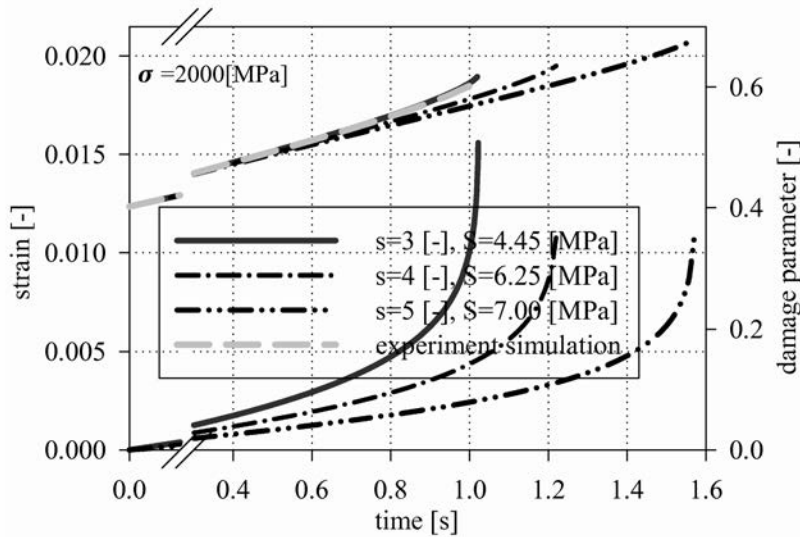
FIG. 8. Creep test for $\sigma = 2000$ [MPa] for different values of damage parameters.

Similarly to the case of a constant strain rate, the damage parameters can be determined on the basis of the creep tests. For that purpose the evolution of the stress and the rate $\dot{p}$ (see Fig. 10) is performed. The parameter S (see Eq. (4.5)) in the Chaboche model calculations without damage are ex-
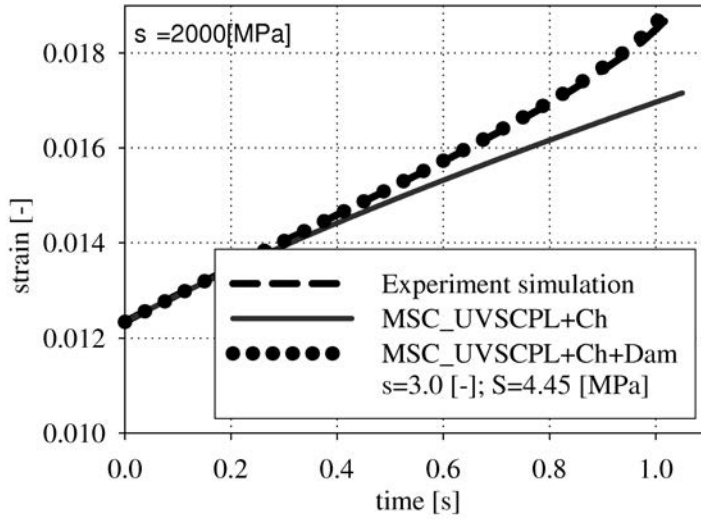
FIG. 9. Creep test for $\sigma = 2000$ [MPa] .
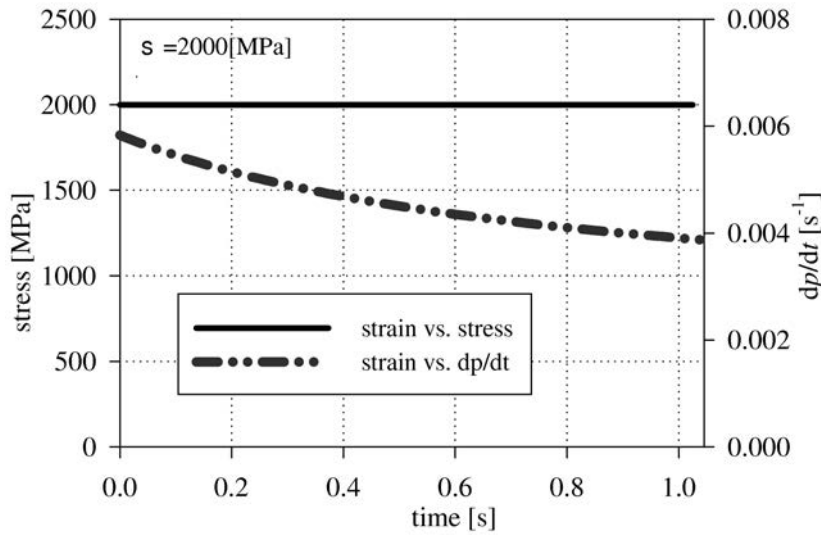
FIG. 10. Stress and $\dot{p}$ in the time domain $\sigma = \text{const} = 2000$ [MPa].

ploited, see Fig. 9 (MSC_UVSCPL+Ch). On the basis of simulation of experiments of the creep test, the rupture times $t_r = 1.045$ [s] (which correspond to $\varepsilon_r^{\text{exp}} = 0.0171$ [–]) are specified. Based on the stress and $\dot{p}$ evolution (see Fig. 10) the first approximation of the parameters $S = 3.98$ [MPa] is calculated for the assumed value of $s = 3.0$ [–]. Next iteration of the numerical analysis gives the final values of $S = 4.45$ [MPa].

4.3. Identification example – direct experiment

In this section the present author identify the damage parameters for steel at 20°C, based on laboratory tests, performed by KŁOSOWSKI [19]. The experimental tests were carried out at the Department of General Mechanics of RWTH Aachen. The following parameters for the basic variant of the Chaboche model are taken for steel (see KŁOSOWSKI [19] for details): $E = 223000$ [MPa], $\nu = 0.3$ [–] and $k = 210.15$ [MPa], $n = 9.51$ [–], $K = 14.085$ [MPas$^{1/n}$], $c = 38840$ [–], $a = 611700$ [MPa], $b = 16.74$ [–], $R_1 = -138.48$ [MPa].

Like in the former case (see preceding section), the damage material parameters for Chaboche model are specified on the basis of the constant strain rate tests. According to the Eq. (4.5) and assuming the value of $s = 2.0$ [–], with the following approximations considered, the parameter $S = 0.4$ [MPa] has been specified.

The results of damage analysis for the estimated damage parameters ($s = 2.0$ [–], $S = 0.4$ [MPa]) with two different strain rates $\dot{\varepsilon} = 0.01$ [s^{-1}] and $\dot{\varepsilon} = 0.001$ [s^{-1}] are given in Figs. 11 and 12. Good agreement has been obtained of strain vs. stress curves from FE calculations and the experiment.

On the basis of numerical simulations the present author has observed that the damage is indicated when the strain is equal to 0.01 [–]. The strains less than 0.01 [–] result in the zero value of the damage parameter D. There is no difference between the results obtained from the numerical simulations with damage (MSC+UVSCPL+Ch+Dam) and without damage (MSC+UVSCPL+Ch), see Fig. 13. This limit specified the strain at the damage threshold.
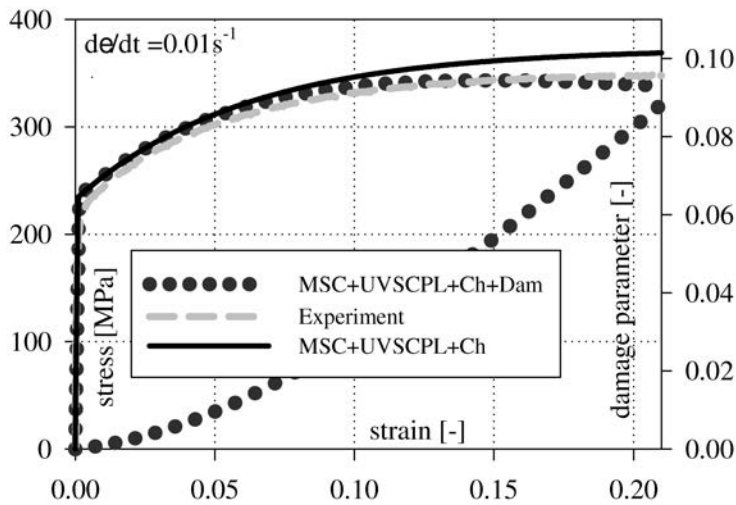
FIG. 11. Numerical simulation of the uniaxial tension test for $\dot{\varepsilon} = 0.01$ [s^{-1}].
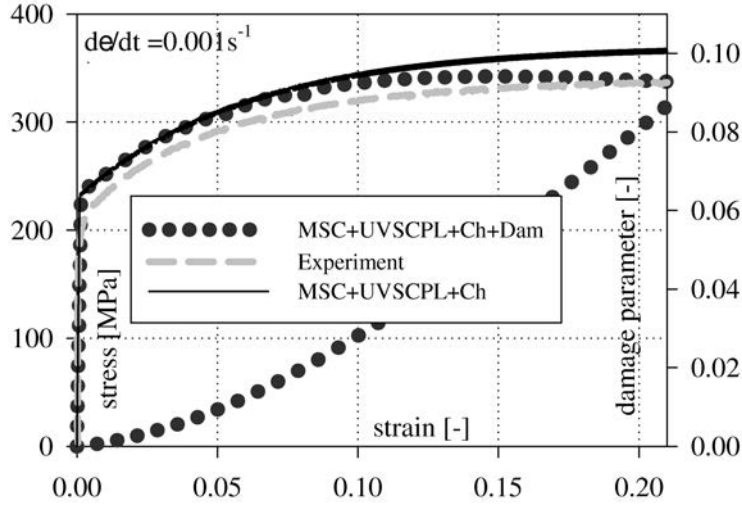
FIG. 12. Numerical simulation of the uniaxial tension test for $\dot{\varepsilon} = 0.001 \left[\text{s}^{-1}\right]$.
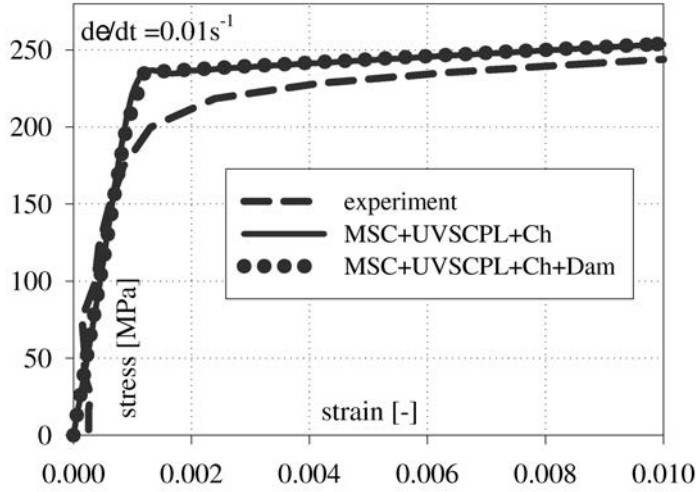
FIG. 13. Numerical simulation of the uniaxial tension test for $\dot{\varepsilon} = 0.01 \left[\text{s}^{-1}\right]$ to the ε_d.

In Table 2 the characteristic values of the ductile damage parameters for three chosen types of steel are given. The strains ε_d and ε_r (see Table 2) specify the strain at damage threshold and strain at failure, and D_c is the critical damage (the value of damage parameter D at macrocracks initiation).

Table 2. Characteristic ductile damage parameters.

Material	ε_d [—]	ε_r [—]	D_c [—]
investigated steel	0.01 [a]	0.45 [b]	0.10 [a]
steel XC 38 [23]	0.00	0.56	0.22
steel 30CD4 [23]	0.02	0.37	0.24
steel E24 [23]	0.50	0.88	0.17

[a] parameters are established on the basis of numerical simulations of uniaxial tensile tests,
[b] parameter is established on the basis of laboratory tests.

5. NUMERICAL EXAMPLES

5.1. Example 1

In this example the numerical analysis of circular steel plate under impact load are investigated. According to symmetry of the structure and loading, a quarter of the plate was analysed. The geometry of the plate used in the numerical calculations is shown in Fig. 14. In the analysis, the four-node shell elements were applied (Element 139, see [34]). The verification was done of the assumed boundary conditions and type of the analysis. For details see [3], where the author described the application of the Bodner–Partom constitutive equations in the finite element analysis.

t [ms]	$p(t)$ [10^5Pa]
0.0	0.00
3.2	0.00
3.5	3.40
4.1	3.40
4.5	4.00
6.0	4.50
11.3	4.60
14.2	5.60
16.0	5.80
24.0	6.05
28.0	6.10
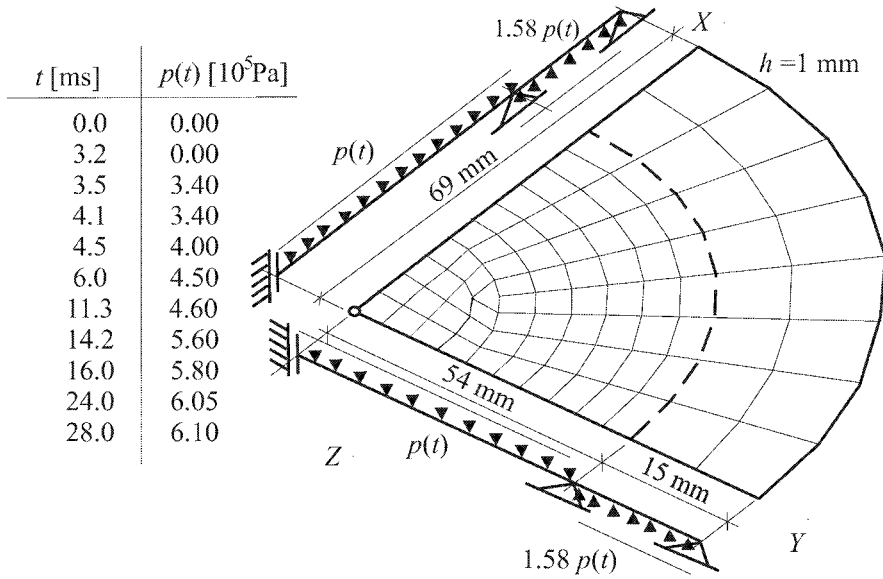
FIG. 14. Circular steel plate subjected to the impact pressure.

For the examined material, the following parameters were assumed: the elastic modulus $E = 223000.0$ [MPa], the Poisson's ratio $\nu = 0.3$ [–]; the thickness of the steel plate $t = 1$ mm. Additionally, the following material parameters for Chaboche model were taken: $k = 210.15$ [MPa], $n = 9.51$ [–], $K = 14.085$ [MPas$^{1/n}$], $c = 38840$ [–], $a = 611700$ [MPa], $b = 16.74$ [–], $R_1 = -138.48$ [MPa], with the damage parameters $s = 2.0$ [–] and $S = 0.4$ [MPa] estimated in the previous section.

The numerical calculations were performed using the proportional damping matrix with the Rayleigh damping multipliers $\alpha = 3.46 \cdot 10^{-6}$ and $\beta = 27.32$. Parameters α and β are the stiffness matrix multiplier and the mass matrix multiplier, respectively. They were calculated by the formula

(5.1)
$$\alpha = 2 \cdot \frac{(\xi_2 \cdot \omega_2 - \xi_1 \cdot \omega_1)}{\omega_2^2 - \omega_1^2},$$
$$\beta = 2 \cdot \omega_1 \cdot \omega_2 \cdot \frac{(\xi_1 \cdot \omega_2 - \xi_2 \cdot \omega_1)}{\omega_2^2 - \omega_1^2},$$

assuming that for the value of critical damping, the first two frequencies were given. The concept of specifying these multipliers is proposed in the paper [7]. To integrate the nonlinear equations of motion, the Newmark algorithm with the time step $\Delta t = 5 \cdot 10^{-7}$ was carried out.

Elasto-viscoplastic Chaboche model with damage is used to describe the behaviour of the steel plate under dynamic vibrations Fig. 15. These results of numerical simulations are compared with the results of the experimental test, which was performed in the impact pipe.
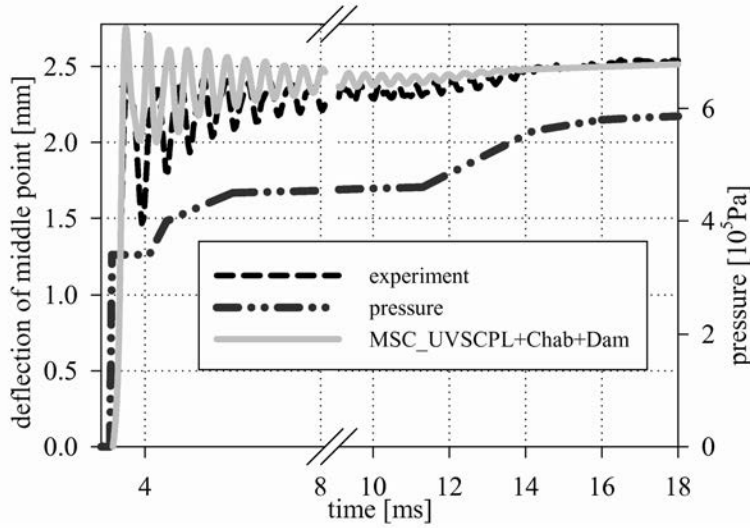
FIG. 15. Inelastic damped vibrations of the plate.

It should be noted that the elastic solution (see Fig. 16) gives a completely different response of the vibrations, while the Chaboche model calculations are close to the experimental results. The maximum value of the damage parameter in this case is about 0.002 [–], thus a non-damage state of the plate is observed. Additionally, the velocity and acceleration plots (Figs. 17, 18) in the time domain illustrate the dynamic behaviour of the plate under impact load.
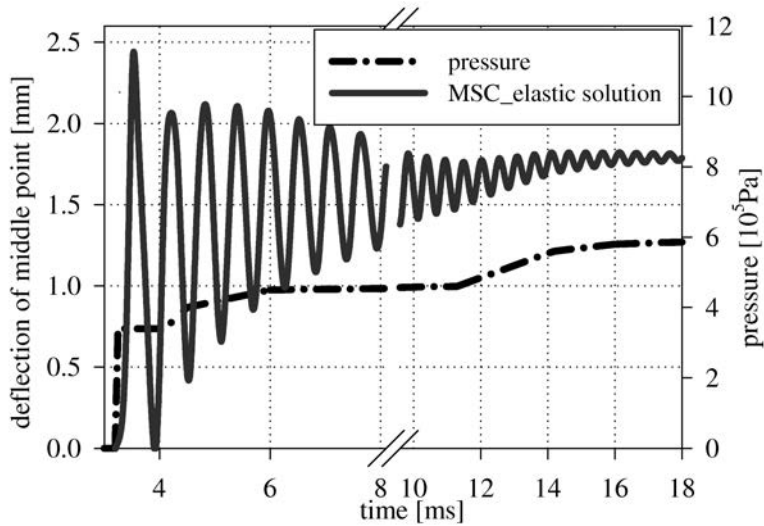

Fig. 16. Elastic damped vibrations of the plate.
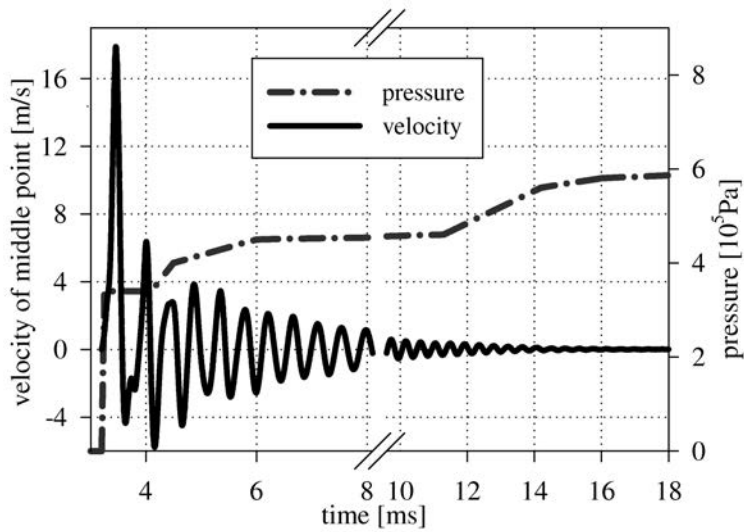
Fig. 17. Middle point velocity.
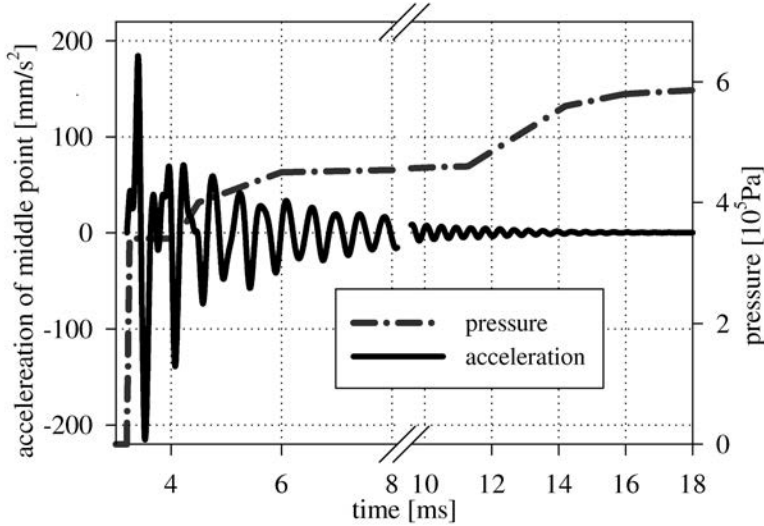
FIG. 18. Middle point acceleration.

5.2. Example 2

At the beginning, the dynamic analysis of a rod subjected to the impact force is presented. The elasto-viscoplastic constitutive equations of the Chaboche model with damage are taken to describe the behaviour of the material. Numerical calculations are performed for a simple truss structure, with the following geometrical parameters: $l = 1.0$ [m] (length) and $A = 0.001$ [m^2] (cross-section area). One of the ends of the rod is fixed while the next end is free. The free end of the truss element is subjected to impact forces F.

The dynamic analysis for three different values of the impact forces $F = 0.10$ [MN] (see Fig. 20), $F = 0.11$ [MN] (see Fig. 21) and $F = 0.12$ [MN] (see Fig. 22) is performed. The force is acting rapidly on the structures, in the time $t = 0.0$ [s], see Fig. 19. For the calculation, the material constants, corresponding to the Chaboche model with the following damage constants were taken (INCO718 at 650°C [2], see also [20]): $E = 159.0$ [GPa], $\nu = 0.3$ [–], $k = 514.21$ [MPa], $b = 60.0$ [–], $R_1 = -194.39$ [MPa], $a = 170000.0$ [MPa], $c = 500.0$ [–], $n = 4.0$ [–], $K = 1023.5$ $\left[(\text{MPa} \cdot \text{s})^{1/n}\right]$, $S = 4.48$ [MPa], $s = 3.0$ [–]. The reference calculations (named MSC_UWSCPL+Ch, see Figs. 20, 21 and 22) were performed without damage, according to the FE procedure given in Fig. 1.

In the research, two variants of the Chaboche model analysis are compared with each other: considering and neglecting the damage. In this case, small influence of damage is observed in the examined time range when the values of

forces are $F = 0.10$ [MN] (see Fig. 20) and $F = 0.11$ [MN] (see Fig. 21). The force $F = 0.12$ [MN] (see Fig. 22) results exceed the limiting damage value, the specimen is destroyed. Evaluation of the damage parameter D, specified by Eq. (2.5), as a function of time, is given in Fig. 23. Due to the merely numerical character of the example, only the calculations for free vibrations are considered. To integrate the nonlinear equations of motion, in the present example the Newmark algorithm [27] with the time step $\Delta t = 5 \cdot 10^{-5}$ [s] is applied.
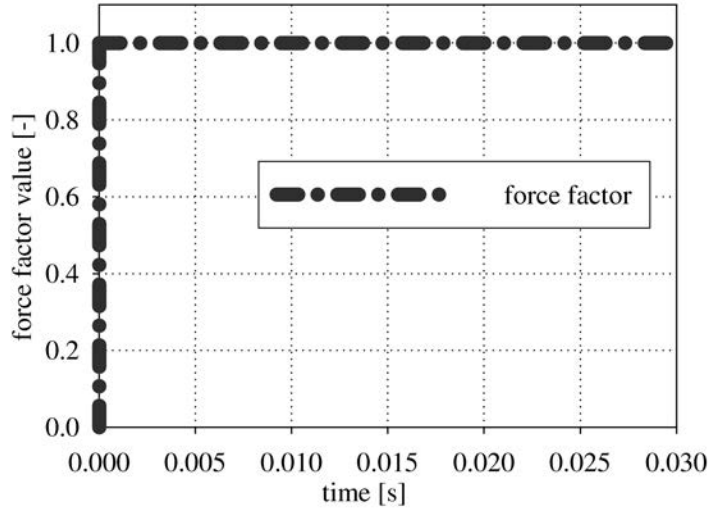
FIG. 19. Force factor value history diagram.
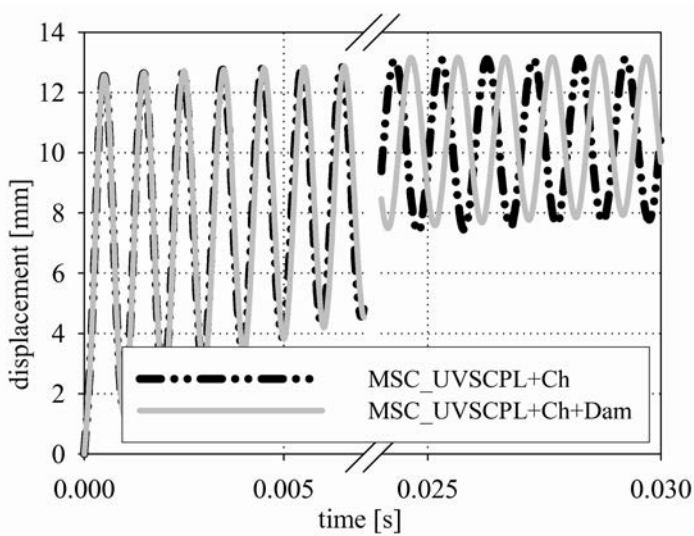
FIG. 20. Displacement diagram for $F = 0.10$ MN.
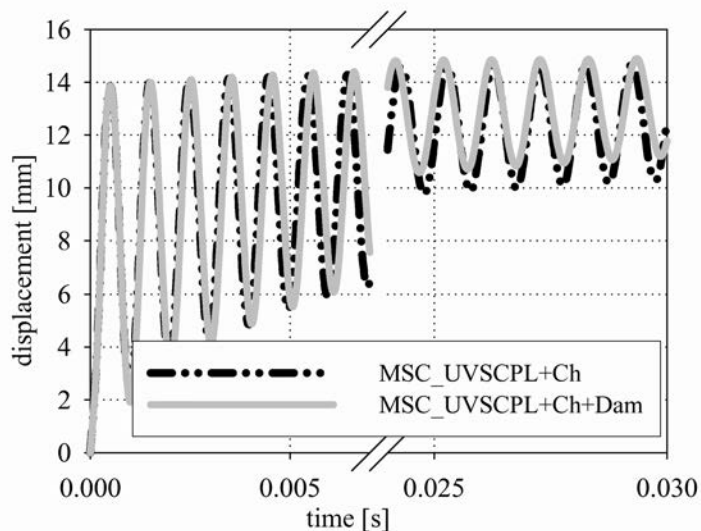
FIG. 21. Displacement diagram for $F = 0.11$ MN.
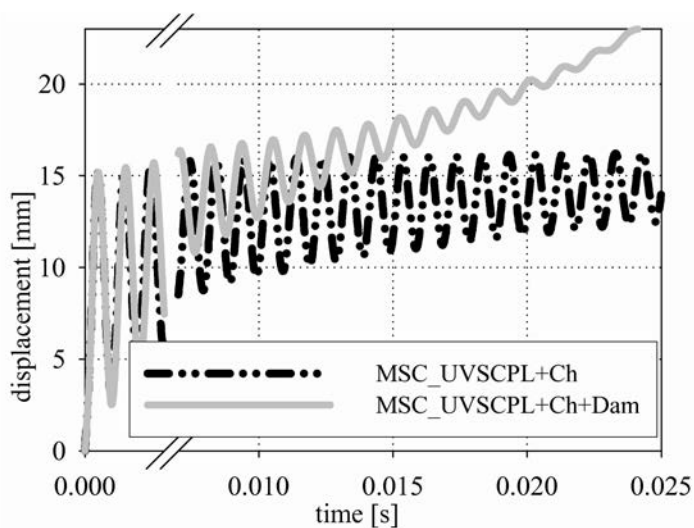
FIG. 22. Displacement diagram for $F = 0.12$ MN.

In the second variant of calculations, geometry of the plate is taken from the Example 1, see Fig. 14. In this case, the material parameters for INCO alloy at 650°C are accepted for the description of the plate material. The evolution of pressure in time domain is accepted according to Fig. 19. High value of the impact pressure, $p = 11.5$ [10^5 Pa], was assumed for distinct presentation of application
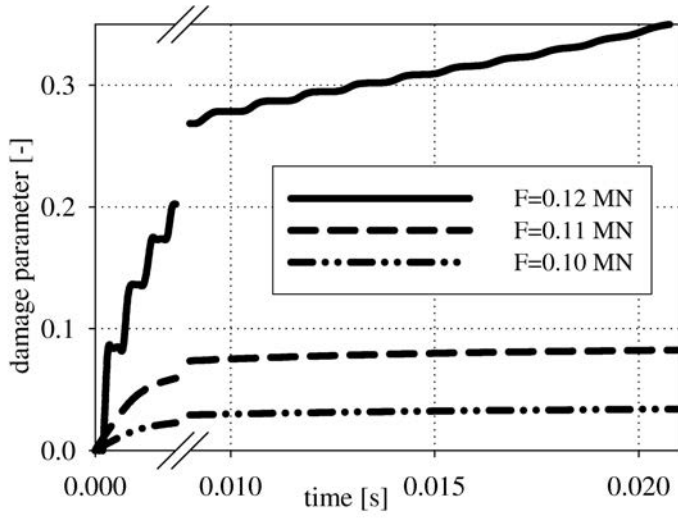
Fɪɢ. 23. Damage parameter evolution.
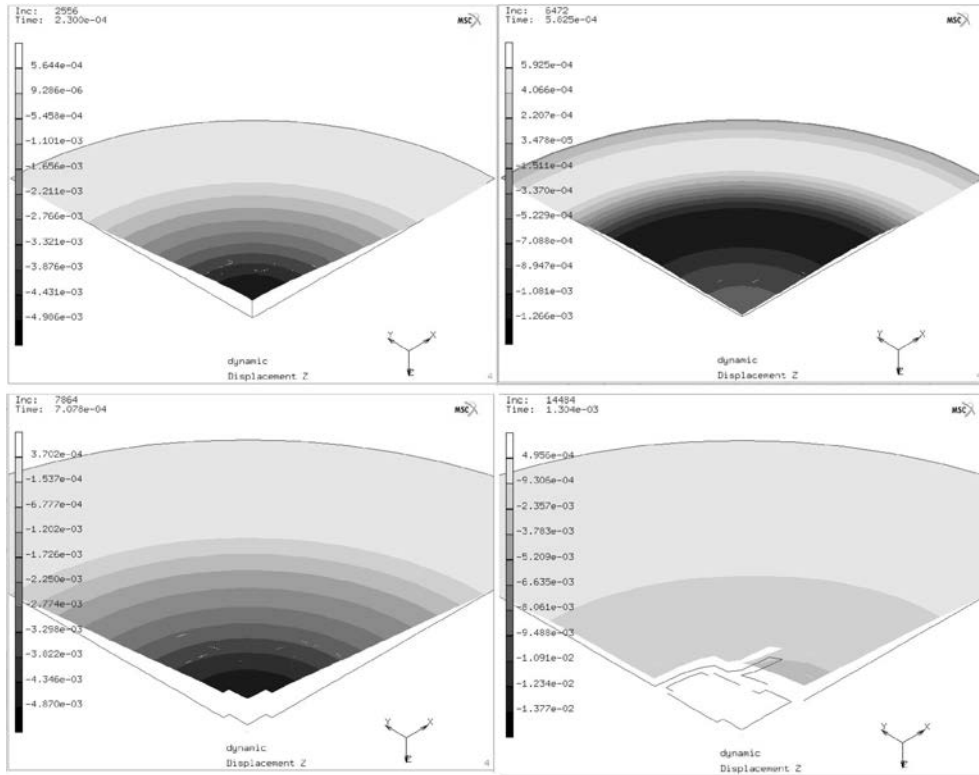
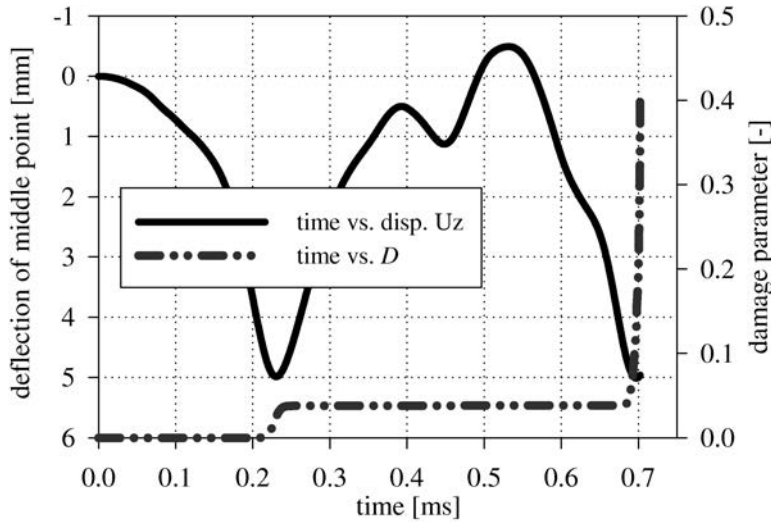Fɪɢ. 24. Damage analysis with UVSCPL+UACTIV subroutines.

Fig. 25. Displacement diagram with damage parameter evolution.

of the proposed procedure for damage analysis. It should be noted that the subroutine UACTIV [34] was used to deactivate elements in the structure model, when the value of the damage parameter D in all integration points of the element is greater than the value of critical damage D_c. The vertical displacements for the quarter of a plate are presented in Fig. 24. The elements close to symmetry lines are deactivated due to evolution of the damage parameters, see Fig. 25. Then the crack runs to a diagonal of the plate. Finally, the middle part of the plate separates and moves rigidly. The author is aware of the fact that the detailed investigation of the structure crack propagation is connected with dynamic crack problems and the knowledge of explosions (see e.g. Nemitz [26], Basista and Nowacki [8] and Włodarczyk [35] for details). Nevertheless, this calculated example demonstrates practical applications of the presented procedure.

6. Conclusions and final remarks

In this study, the author proposed an improved concept of identification and validation of damage parameters. A model of isotropic damage based on a continuum damage variable on the concept of effective stress, can be directly applied in calculations. The procedures are presented to introduce the Chaboche model considering damage, into the open commercial FE-program code. Identification is made for nickel-based superalloy INCO718 and for steel by means of elastic modulus change caused by damage. The numerical examples prove that the Chaboche law and the presented method of performing the numerical implementation, are

effective. The future research should be concentrated on the development of the FE procedure, with emphasis placed on temperature influences and criterion for crack extension.

It is worth pointing out that the presented damage approach with the concept of damage parameters identification has been successfully used by the present author to describe the damage evaluation in the elasto-viscoplastic constitutive equations of the Bodner–Partom model, (for details see [5]).

References

1. J. Aktaa, B. Schinke, *Unified modelling of time dependent damage taking into account an explicit dependency on backstress,* International Journal of Fatigue, **19**, 3, 195–200, 1997.

2. G. Amar, J. Dufailly, *Identification of viscoplastic and damage constitutive equations*, European Journal of Mechanics, **12**, 2, 197–218, 1985.

3. A. Ambroziak, *Application of elasto-viscoplastic Bodner-Partom constitutive equations in finite element analysis*, Computer Assisted Mechanics and Engineering Sciences (in press).

4. A. Ambroziak, *Chaboche model – development and FE application*, Zeszyty Naukowe Politechniki Śląskiej, **104**, 35–42, 2005.

5. A. Ambroziak, *Modelling of continuum damage for application in elasto-viscoplastic Bodner-Partom constitutive equations*, Engineering Transactions (in press).

6. A. Ambroziak, *Numerical modelling of elasto-viscoplastic Chaboche constitutive equations using MSC. Marc*, Task Quarterly, **9**, 2, 157–166, 2005.

7. A. Ambroziak, *Viscoplastic analysis of damped vibrations of circular plate, [in:] Shell Structures: Theory and applications*, W. Pietraszkiewicz and C. Szymczak [Eds.], Taylor and Francis, London, 445–449, 2005.

8. M. Basista, W.K. Nowacki [Eds.] *Modelling of damage and fracture processes in engineering materials*, In Series: Trends in Mechanics of Materials. Volume 2, IPPT PAN, Warsaw 1999.

9. A. BERTRAM, J. OLSCHEWSKI, *Anisotropic creep modelling of single crystal superalloy SRR99,* Journal of Computational Mathematic Science, **5**, 12–16, 1996.

10. S.R. BODNER, Y. PARTOM, *Constitutive equations for elastic-viscoplastic strain-hardening materials*, Journal of Applied Mechanics, ASME, **42**, 385–389, 1975.

11. W. BROCKS, R. LIN, *An extended Chaboche viscoplastic law at finite strains and its numerical implementation*, GKSS-Forschunszentrum Geesthacht GmbH, Geesthacht 2003.

12. J.-L. CHABOCHE, *Constitutive equations for cyclic plasticity and cyclic viscoplasticity*, International Journal of Plasticity, **5**, 247–302, 1989.

13. J.-L. CHABOCHE, G. ROUSSELIER, *On the plastic and viscoplstic constitutive equations*, International Journal of Pressure Vessels and Pining, **105**, 105–164, 1983.

14. P. FOTIU, H. IRSCHIK, F. ZIEGLER, *Material science and numerical aspects in the dynamics of damaging structures*, [in:] Structural dynamics, G.I. SCHUELER [Ed.], Springer-Verlag, New York, 235–255, 1991.

15. T. FURAKAWA, G. YAGAWA, *Inelastic constitutive parameter identification using an evolutionary algorithm with continuous individuals*, International Journal for Numerical Methods in Engineering, **40**, 1071–1090, 1997.

16. D.R. HAYHURST, F.A. LECKIE, *The effect of creep constitutive and damage relations upon the rapture time of a solid circular torsion bar*, Journal of the Mechanics and Physics of Solids, **21**, 431-446, 1973.

17. L.M. KACHANOV, *Introduction to continuum damage mechanics*, Martinus Nijhoff Publishers, Dordecht, 1986.

18. L.M. KACHANOV, *Time of rapture process under creep conditions*, TVZ Akad. Nauk. S.S.R. Otd. Tech. Nauk., **8**, 26–31, 1958.

19. P. KŁOSOWSKI, *Nonlinear numerical analysis and experiments on vibrations of elasto-viscoplastic plates and shells* [in Polish], Politechnika Gdańska, Gdańsk 1999.

20. P. KŁOSOWSKI, K. WOZNICA, *Comparative analysis of dynamic behaviour of an elasto-viscoplastic truss element*, Machine Dynamics Problems, **24**, 3, 33–53, 2000.

21. F.A. LECKIE, *The constitutive equations of continuum creep damage mechanics*, Philosophical Transactions of the Royal Society of London, **288**, 27–47, 1978.

22. J. LEMAITRE, *Micro-mechanics of crack initiation*, International Journal of Fracture, **42**, 247–302, 1989.

23. J. LEMAITRE, *A continuous damage mechanics. Model for ductile fracture*, Journal of Engineering Materials and Technology, **107**, 83–89, 1985.

24. J. LEMAITRE, *A course on damage mechanics*, Springer-Verlag, New York 1992.

25. J. LEMAITRE, A. PLUMTREE, *Application of damage concept to predict creep-fatigue failures*, Journal of Engineering Material and Technology, **101**, 284–292, 1979.

26. A. NEMITZ, *Crack mechanics* [in Polish], PWN, Warsaw 1998.

27. N.M. NEWMARK, *A method of computation for structural dynamics*, Journal of the Engineering Mechanics Division, **85**, 67–94, 1959.

28. W.K. NOWACKI, J.R. KLEPACZKO [Eds.], *New experimental methods in material dynamics and impact.* in Series: Trends in Mechanics of Materials, Volume 3, IPPT PAN and CoE AMAS, Warsaw 2001.

29. P. Perzyna, *Fundamental problems in viscoplasticity*, Advanced in Mechanics, **9**, 243–377, 1966.

30. W. Qi, W. Brock, *ABAQUS user subroutines for simulation of viscoplastic behaviour including anisotropic damage for isotropic materials and for single crystals*, Technical Note GKSS/WMS/01/5, GKSS-Forschunszentrum Geesthacht GmbH, Geesthacht 2001.

31. Y.N. Rabotnov, *Creep problems of structural members*, North-Holland, Amsterdam, 1969.

32. J.C. Simo, J.W. Ju, *Strain- and stress-based continuum damage models*, International Journal of Solids and Structures, **23**, 7, 821–869, 1987.

33. J. Skrzypek, H. Kuna-Cisałka, A. Garncarski, *Continuum damage mechanics modelling of creep-damage and elastic-damage-fracture in materials and structures*, [in:] *Modelling of damage and fracture processes in engineering materials*, Basista M., Nowacki W.K. [Eds.], Institute of Fundamental Technology Research Polish Academy of Science, Warsaw 1999.

34. Users handbook MSC.MARC, Volume B: Element library; Volume D: User subroutines and special routines, Version 2003, MSC. Software Corporation, 2003.

35. E. Włodarczyk, *Introduction to mechanic of explosion* [in Polish], PWN, Warsaw 1994.

36. K. Woznica, *Dynamique des structures elasto-viscoplastiques*, Cahiers de Mécanique, Lille 1998.

37. A. Ambroziak, P. Kłosowski, *Survey of modern trends in analysis of continuum damage in mechanics*, Task Quarterly, **10**, 4, 437–454, 2006.

38. A. Ambroziak, P. Kłosowski, M. Nowicki, R. Schmidt, *Implementation of continuum damage in elasto-viscoplastic constitutive equations*, Task Quarterly, **10**, 2, 207–220, 2006.